Journal of Solid State Chemistry 183 (2010) 1209–1214

Contents lists available at ScienceDirect

Journal of Solid State Chemistry

journal homepage: www.elsevier.com/locate/jssc

Sol–gel synthesis of mesoporous $CaCu_3Ti_4O_{12}$ thin films and their gas sensing response

R. Parra [a,*], R. Savu [b], L.A. Ramajo [a], M.A. Ponce [a], J.A. Varela [b], M.S. Castro [a], P.R. Bueno [b], E. Joanni [b,c]

[a] Instituto de Investigaciones en Ciencia y Tecnología de Materiales (INTEMA), CONICET-UNMdP, J. B. Justo 4302, B7608FDQ Mar del Plata, Argentina
[b] Instituto de Química, UNESP, Rua F. Degni s/n, 14800-900 Araraquara, SP, Brazil
[c] Centro de Tecnologia da Informação Renato Archer, Rodovia Dom Pedro I (SP-65) km 143,6, 13069-901 Campinas, SP, Brazil

ARTICLE INFO

Article history:
Received 18 January 2010
Received in revised form
26 March 2010
Accepted 26 March 2010
Available online 1 April 2010

Keywords:
$CaCu_3Ti_4O_{12}$
Mesoporous films
Gas sensors

ABSTRACT

A new sol–gel synthesis procedure of stable calcium copper titanate ($CaCu_3Ti_4O_{12}$—CCTO) precursor sols for the fabrication of porous films was developed. The composition of the sol was selected in order to avoid the precipitation of undesired phases; ethanol was used as solvent, acetic acid as modifier and poly(ethyleneglycol) as a linker agent. Films deposited by spin-coating onto oxidized silicon substrates were annealed at 700 °C. The main phase present in the samples, as detected by X-ray diffraction and Raman spectroscopy, was $CaCu_3Ti_4O_{12}$. Scanning electron microscopy analysis showed that mesoporous structures, with thicknesses between 200 and 400 nm, were developed as a result of the processing conditions. The films were tested regarding their sensibility towards oxygen and nitrogen at atmospheric pressure using working temperatures from 200 to 290 °C. The samples exhibited n-type conductivity, high sensitivity and short response times. These characteristics indicate that CCTO mesoporous structures obtained by sol–gel are suitable for application in gas sensing.

1. Introduction

Calcium copper titanate ($CaCu_3Ti_4O_{12}$—CCTO) has attracted widespread attention since the large dielectric constant ε of bulk samples was first reported in 2000 [1,2]. The origin of the exceptional dielectric constant value for this non-ferroelectric material has been attributed to grain boundary capacitance and extrinsic defects rather than to intrinsic properties associated to the crystalline structure [2–4]. Despite the diverse ε values reported in the literature, ranging form 10^2 to 10^5, CCTO is a promising material for electroceramic devices such as capacitors [3–5], gas sensors [6–8] and varistors [9,10].

CCTO ceramics are generally synthesized by the mixed oxide route [2,9–13]. For thin films, the most usual methods are MOCVD [5], physical methods such as pulsed laser deposition (PLD) [6] and sputtering [7], and solution methods [14,15]. It is said that the synthesis from solutions leads to uniform mixing at atomic scale, yielding homogeneous materials. However, obtaining pure CCTO at temperatures below 1000 °C by traditional ceramic processing techniques and solution procedures is very difficult. Recently, the sol–gel synthesis has been also put into practice due to its cost-effectiveness and high versatility [16–27]. The technique allows the deposition of both dense and porous ceramic films and does not require expensive vacuum equipment. Surprisingly, not much attention has been paid to the chemistry of CCTO-precursor sols, in spite of the fact that precipitation of undesired species might easily occur before film deposition. The effect of solvents, precursors, modifiers, coordinating agents and the side reactions that may occur in solution need to be considered in order to synthesize stable sols of a composition as complex as CCTO. Apart from the sintering temperature, this set of factors will determine film quality, crystallization of different phases, grain size distribution and the degree of porosity of the resulting films.

Most of the studies on CCTO focus on the dielectric property of bulk ceramics and dense films. Nevertheless, calcium copper titanate has also demonstrated advantages for gas sensing applications in the form of polycrystalline porous nanostructures, but very few works have been published since it is a relatively new material. The detection and monitoring of gases and toxic species is currently one of the most actively investigated subjects. Research is being carried out to develop more sensitive and selective gas, chemical- and bio-sensors. Oxygen sensors, which are widely used in automobile gas exhausts for O_2 partial pressure monitoring, are among the most widely spread commercial applications with environmental interest [6]. Interestingly, Tuller et al. used PMMA microspheres as templating agents for CCTO gas-sensing films deposited by PLD [6]. The fabrication of sputtered CCTO porous films with high gas sensitivity has been recently reported by our group [7]. It has been shown that, depending on the synthesis method and experimental conditions,

* Corresponding author.
E-mail address: rparra@fi.mdp.edu.ar (R. Parra).

0022-4596/$ - see front matter © 2010 Elsevier Inc. All rights reserved.
doi:10.1016/j.jssc.2010.03.033

n or p type conductivity can be attained [6,7]. To date, the chemical synthesis of CCTO porous films has not been reported. In this paper, we put forward a sol–gel synthesis procedure for mesoporous CCTO films with potential for gas sensing applications. We also propose a discussion on the chemical composition of the CCTO-precursor sol regarding undesired effects of solvents, complexing agents and templates usually employed in the synthesis of CCTO by sol–gel methods.

2. Materials and methods

The $CaCu_3Ti_4O_{12}$ precursor sol was prepared as follows: copper ($Cu(NO_3)_2 \cdot 2.5H_2O$; Aldrich 99.99%) and calcium nitrates ($Ca(NO_3)_2 \cdot 4H_2O$; Riedel-de Haën 99%) were dissolved in absolute ethanol (Merk, $>99.5\%$) with the addition of glacial acetic acid (Merk, 100%). The solution was heated for 2 h under reflux in a silicon oil bath at 80 °C. Simultaneously, titanium tetraisopropoxide ($Ti(O^iPr)_4$; Alfa Aesar 99.995%) was mixed with glacial acetic acid and stirred inside a sealed vial for 2 h. Finally, the copper and calcium solution was added slowly to titanium solution under constant stirring. The translucent blue sol, protected from ambient moisture, did not gel neither showed the formation of precipitates after an aging period of 30 days. A detailed flow diagram of the experimental procedure is shown in Fig. 1. Notice the high concentration of the sol.

Before film depositions, the sol was modified by the addition of poly(ethyleneglycol) of 400 Da (PEG400). Ethanol was also included in the sols with the objective of increasing porosity. Although the water present in Ca and Cu salts is sufficient for hydrolysis to occur, deionized water was added in order to promote condensation and the formation of a Ti–O-based network with the accompanying increase in viscosity. The final compositions of sols prepared using different amounts of PEG400 (CCTO90 and CCTO120) are shown in Fig. 1.

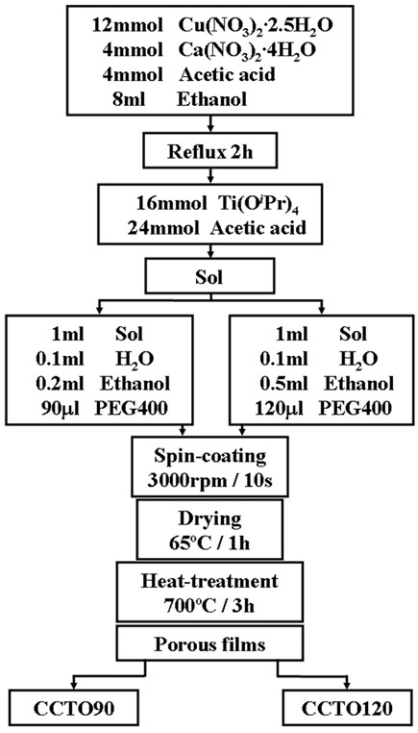

Fig. 1. Detailed flow chart for the sol–gel synthesis and films deposition procedures.

Films were deposited 30 min after water addition by spinning the modified sols under ambient atmospheric conditions onto Si/SiO_2 substrates at 3000 rpm for 10 s using a Laurell WS400-E spin processor. The as-fabricated layers were immediately placed in an oven at 65 °C for 1 h for solvent evaporation and were subsequently annealed at 700 °C for 3 h in a tubular furnace, using heating and cooling rates of 5 °C/min.

The crystalline phases present in heat-treated films were assessed by X-ray diffraction (XRD; Rigaku 20000) under Cu$K\alpha$ radiation in a low angle of incidence. In order to confirm phase formation, micro-Raman spectroscopy was performed at room temperature by means of a Renishaw inVia microscope. The 514 nm Ar ion laser line (50 mW nominal power) was used as excitation and the signal was dispersed by a diffraction grating having 2400 lines/mm. The microstructural characterization of sintered films was carried out by means of field emission scanning electron microscopy (FE-SEM; Zeiss Supra 35).

For registering the gas sensing response towards oxygen, platinum electrodes with thicknesses of 150 nm were sputtered onto the sintered films at 200 °C, 2×10^{-2} mbar and a DC power of 50 W. The electrodes were deposited in a planar configuration achieved with a shadow mask, giving rise to a 2 mm gap between them. The films were tested in a custom-made chamber with a volume of 165 cm^3 with an accurate control of working temperature, pressure, gas flow and composition. Electrical resistance measurements were carried out at 220 and 290 °C with an HP4192A impedance analyzer in the 40 Hz–110 MHz frequency range. In the test procedure, the chamber was filled with 100 sccm (square cubic centimeters per minute) of N_2 and the devices were heated to the desired temperature. After the temperature stabilized, 100 sccm of pure O_2 were injected into the chamber and the measurements were initiated. The changes in the sensor electrical resistance were recorded at a frequency of 40 Hz applying a 5 V dc bias.

3. Results and discussion

3.1. Sol composition

In a recent paper we reported on the photoluminescent response of CCTO-based films prepared from a CCTO-precursor sol [22]. Several modifications were made to that synthesis procedure in order to obtain sols having long-term stability for CCTO films and bulk devices. For instance, copper and calcium nitrates are more easily dissolved in absolute ethanol ($\varepsilon \sim 24.3$ at 25 °C) than in 2-propanol ($\varepsilon \sim 18.3$ at 25 °C). In the latter solvent copper nitrate (hemipentahydrate) rapidly formed a very fine white solid that could be filtered and identified as copper hydroxynitrate $Cu_4(OH)_6(NO_3)_2$ (JCPDS 74-1749) by means of the XRD pattern shown in Fig. 2a. Concerning 2-methoxyethanol, it is a known toxic compound whose use should be avoided because of its teratogenic effects and birth defect risks.

The use of acetic acid for preparation of the copper/calcium solution reported in this study improved salt solubilization and prevented $Cu_4(OH)_6(NO_3)_2$ precipitation. Copper hydroxynitrate formation proceeds according to the following reaction:

$$4Cu(NO_3)_2 \cdot 2.5H_2O \xrightarrow{2\text{-propanol}} Cu_4(OH)_6(NO_3)_2 + 6NO_3^- + 6H^+ + 4H_2O \quad (1)$$

One disadvantage of ethanol with respect to 2-propanol is the higher esterification rate with acetic acid in the presence of a weak Lewis acid (Ti(IV)) that catalyzes the reaction. Esterification reactions produce water as a byproduct and promote the hydrolysis and condensation of titanium tetraisopropoxide leading to a TiO_2 gel with Ca and Cu ion species distributed within the Ti–O–Ti network. Besides, the presence of water also contributes

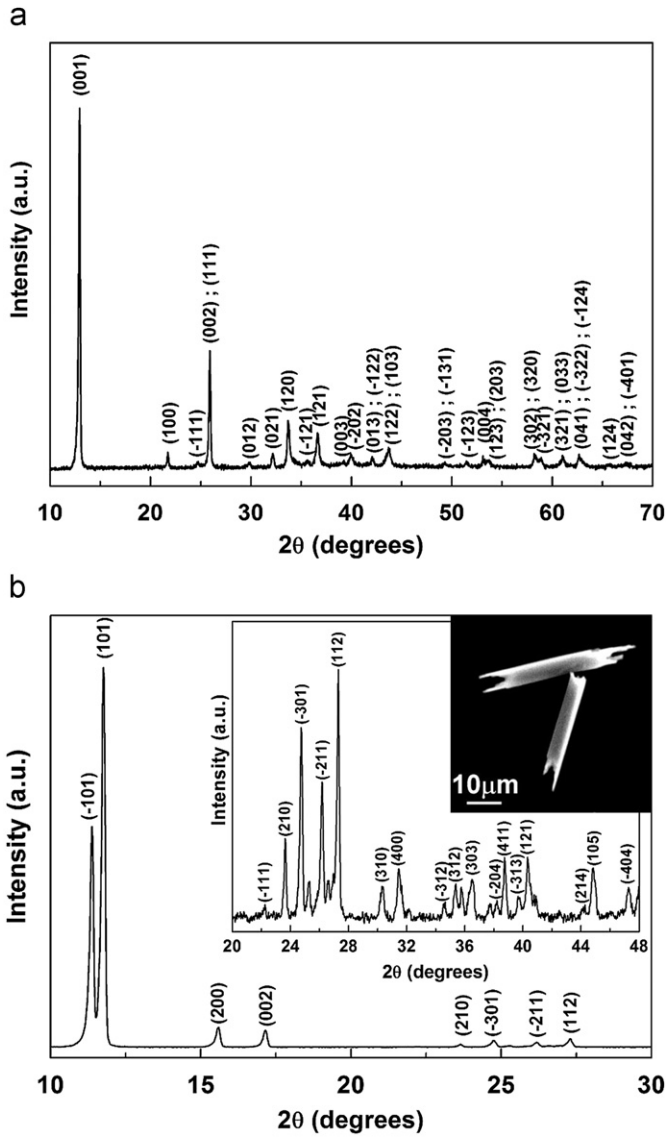

Fig. 2. (a) XRD pattern of the solid formed in $Cu(NO_3)_2 \cdot 2.5H_2O$ and $Ca(NO_3)_2 \cdot 4H_2O$ in 2-propanol solutions corresponding to $Cu_4(NO_3)_2(OH)_6$. (b) XRD pattern of $Cu(acac)_2$ needles formed in $Ti(O^iPr)_4$, $Cu(NO_3)_2 \cdot 2.5H_2O$, $Ca(NO_3)_2 \cdot 4H_2O$ and acetylacetone solutions. Inset shows a magnification of the 20–48° 2θ region and a SEM image of large $Cu(acac)_2$ rod-like crystals.

to the precipitation of Cu(II) hydroxide and/or hydroxynitrate. Nevertheless, no such effects were observed in the ethanol-based solution, even after several days.

It was also observed that in this particular case, acetic acid resulted a more appropriate modifier to $Ti(O^iPr)_4$ than 2,4-pentanodione (acetylacetone or acac). Chemical modification is necessary because it slows down gelation and, especially, the uncontrolled precipitation of TiO_2 after water addition [28]. Acetylacetone, the simplest of β-diketones, is among the most used chelating agents. It is known to form neutral chelates with a great number of metal ions. The addition of 1 mol of acac to 1 mol of $Ti(O^iPr)_4$ leads to a $Ti(O^iPr)_3$ acac complex, which, on addition of a large water excess, forms a long-term stable 3D nanocrystalline colloidal sol [29]. Unfortunately, in the presence of acac, copper forms the stable chelate copper(II) acetylacetonate ($Cu(acac)_2$), which precipitates from the solution. This complex precipitated in the form of grey-blue rods from a 1:1 (molar ratio) $Ti(O^iPr)_4$:acac (Aldrich, $>99.9\%$) sol to which an ethanolic solution of calcium and copper nitrates, in the stoichiometric amounts required for CCTO, had been previously added. The rods were left to grow for 2 days, filtered, washed with ethanol and characterized by XRD and SEM as shown in Fig. 2b. The diffraction pattern coincides with the JCPDS 11-800 file for $Cu(acac)_2$ or $Cu(C_5H_7O_2)_2$. Then, the formation of copper hydroxynitrate and copper acetylacetonate in the CCTO-precursor sol can be avoided by dissolving copper nitrate in absolute ethanol with the addition of glacial acetic acid and by modification of $Ti(O^iPr)_4$ with acetic acid.

Impurities and heterogeneities may also occur in the films due to inorganic phase separation during film drying. As suggested by Sanchez et al. [30], when more than one type of inorganic precursor or metals in different oxidation states are used, the formation and stabilization of the inorganic/organic layer must be completed before the inorganic network is consolidated. According to this, PEG400 was added to the sol few minutes before water was added and, in order to avoid inorganic phase separation due to differences in solubility, the films were immediately *freezed* for consolidation of the inorganic structure by introducing them into an oven at 65 °C after spinning. The films thus prepared consist of hybrid xerogels with PEG400 embedded in the inorganic matrix [30]. The subsequent thermal treatment allows decomposition of the organic polymer, condensation and crystallization of, ideally, single-phase CCTO.

Beside numerous defects that may occur in films deposited by spin-coating, the formation of comet-shaped inhomogeneities is caused by the presence of solid particles in sols (also by deficient substrate cleaning) that obstruct the flow of the sol over the substrate [31]. Moreover, the precipitation of undesired compounds must be avoided throughout the synthesis process since it leads to the heterogeneous distribution of species in the final coating and to the formation and growth of large amounts of particles of secondary phases. These heterogeneities are an impediment to CCTO phase formation that will ultimately have an effect on the film quality and electrical performance of the devices.

3.2. Structural properties of sintered films

Figs. 3 and 4 show the surface (Figs. 3a and 4a) and cross-section (Figs. 3b and 4b) FE-SEM images of the CCTO90 and CCTO120 films, respectively, after heat treatment at 700 °C for 3 h.

Both films show good adhesion to the substrate and consist of homogeneous and crack-free microstructures formed of interconnected nanoparticles. The majority of pores are in the mesoscale range with sizes between 25 and 50 nm, though larger pores (100–200 nm) could also be observed. The CCTO90 composition led to a film thickness of 200 nm (Fig. 3b), whereas the CCTO120 had a thickness of approximately 400 nm (Fig. 4b). Interestingly, the films are quite thick; this is attributed to the porosity but, also, to the high concentration of the precursor sol and to the increase in the sol viscosity after PEG and water addition.

In the FE-SEM images it is obvious that the porosity increased with the higher dilution or solvent (ethanol) content and with the addition of poly(ethyleneglycol). It has been established that larger pores are formed with higher PEG concentrations as well as with the use of PEG of higher average molecular weights [30,32,33]. Moreover, the formation of an inorganic–organic polymer by the association of oxygen in PEG to Ti centers confers flexibility to the structure and prevents the film from cracking during drying. For preparing sample CCTO120, the sol was diluted to 50% with ethanol and also a higher amount (30%) of PEG was

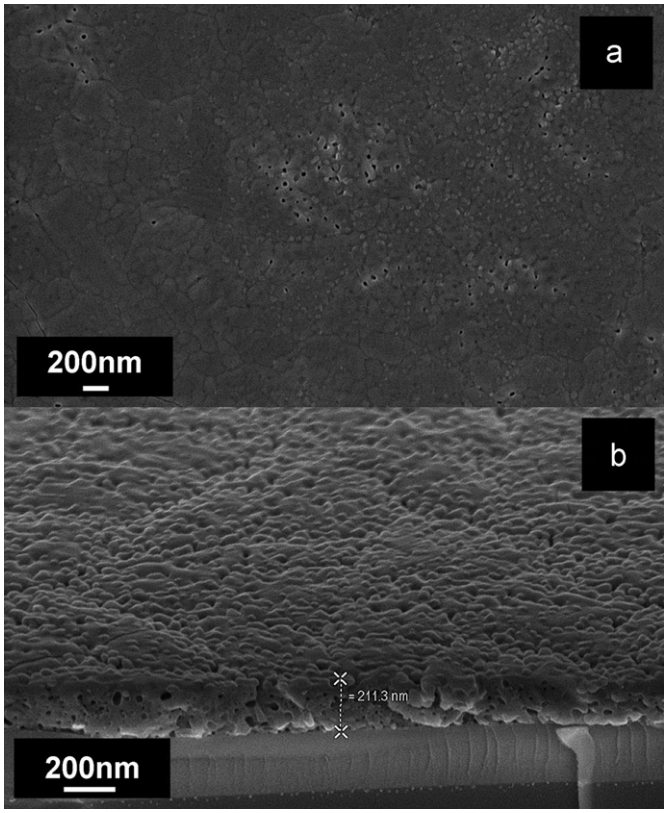

Fig. 3. Surface (a) and cross-section (b) FE-SEM images of the CCTO90 mesoporous film sintered at 700 °C for 3 h.

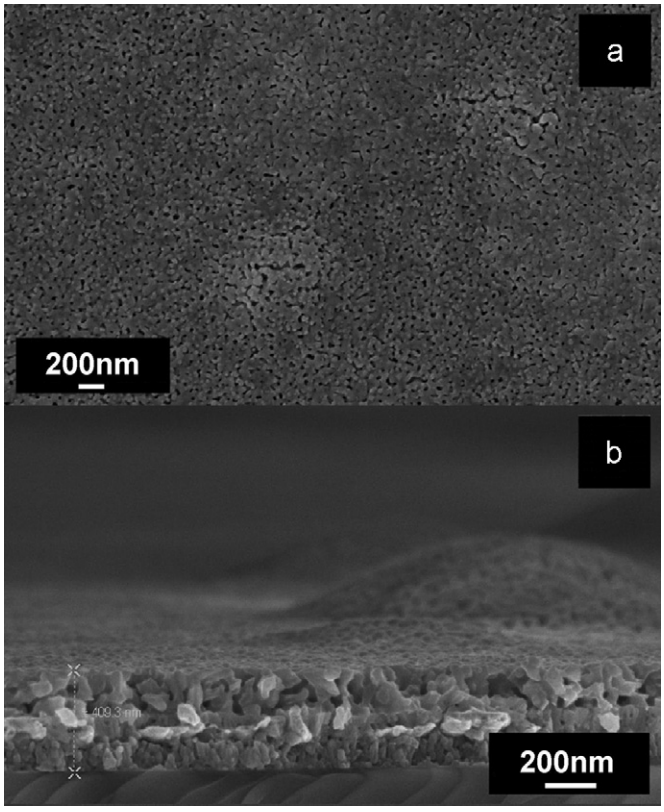

Fig. 4. Surface (a) and cross-section (b) FE-SEM images of the CCTO120 mesoporous film sintered at 700 °C for 3 h.

added with respect to sample CCTO90. This led to a considerable increase in thickness, porosity and mainly, to a more open film structure having a high surface-to-volume ratio. All these characteristics are desirable for gas sensing devices based on thin films.

As the CCTO120 film presented better structural characteristics for gas-sensing films, further characterizations were performed in order to evaluate its crystallinity and morphology. The XRD pattern in Fig. 5 corresponds to this film sintered at 700 °C, confirming that CCTO is the main phase crystallizing at this temperature.

Although rutile TiO_2 (JCPDS 74-2485) is the only minority phase that could be undoubtedly detected in the XRD pattern, based on previous work [22], the presence of small quantities of $CaTiO_3$ and CuO was not, *a priori*, disregarded in these films. Nevertheless, the Raman spectra (Fig. 6) obtained from the CCTO120 film surface showed the bands associated with the active modes expected both for CCTO and the rutile phase of TiO_2 (250 and 610 cm^{-1}) [34].

According to the studies reported by Kolev et al. [35] and Valim et al. [36], the bands near 290, 445 and 510 cm^{-1} are associated to TiO_6 rotation-like modes, whereas the bands at 574 cm^{-1} and around 780 cm^{-1} are characteristic for Ti–O–Ti antistretching and stretching vibrations of TiO_6 octahedra, respectively. The band of Si due to the substrate is evident at 521 cm^{-1}, but Raman active modes associated with calcium

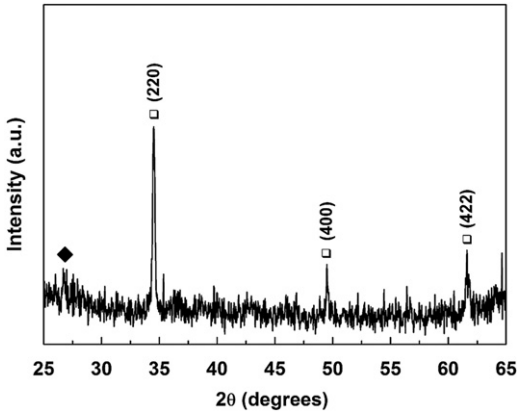

Fig. 5. XRD pattern of the CCTO120 heat-treated film at 700 °C (❑ $CaCu_3Ti_4O_{12}$; ◆ TiO_2).

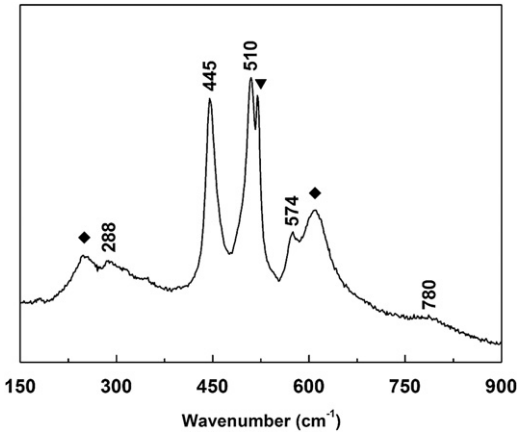

Fig. 6. Raman spectrum of the CCTO120 film showing bands assigned to $CaCu_3Ti_4O_{12}$. Active modes due to rutile TiO_2 (◆) and Si (▼) are also indicated.

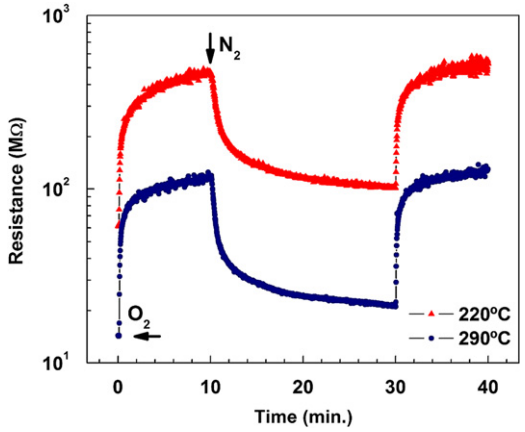

Fig. 7. Gas sensing response (electrical resistance vs. time) towards O_2 for the CCTO120 sample. The measurements were carried out at 220 and 290 °C and 40 Hz frequency, applying a 5 V difference potential.

titanate or copper oxides, as reported in the literature, are not noticeable in the spectrum [37,38]. This is in good agreement with the XRD pattern and confirms that $CaCu_3Ti_4O_{12}$ is the main phase in these films with rutile TiO_2 present only as a minor impurity.

3.3. Gas sensing properties

The gas sensing response towards oxygen for the CCTO120 film is presented in Fig. 7. The highly porous structure and elevated surface-to-volume ratio favors the diffusion of gases into the film, enhancing the sensor response.

The variation of sensor electrical resistance (R) as a function of time was measured for two oxygen–nitrogen cycles at both 220 and 290 °C working temperatures. As expected, a decrease in R when the temperature was increased from 220 to 290 °C took place due to the fact that current transport mechanisms in oxides are promoted by temperature. As shown in Fig. 7, at 290 °C the resistance reaches an almost steady state in a shorter time than for 220 °C. The response time of a semiconducting gas sensor is based on the reactivity and diffusion of gas molecules inside the sensing layer [39], these processes being once again enhanced with temperature. When the target gas was injected into the chamber, the adsorption of O_2 onto the film surface led to a sudden increase in resistance, indicating n-type conduction, in agreement with previous work [6]. The device exhibits reproducible response and recovery times for both testing temperatures. Stabilization was faster at 290 °C with the resistance increasing by almost one decade for this temperature. For both temperatures, the higher electrical resistance value registered after the recovery time ended (in nitrogen) can be related to a higher voltage barrier and to a reduction of the donor concentration.

Based on the XRD and Raman spectroscopy analysis, which indicated the CCTO as principal crystalline phase, the electrical response to modifications in the surrounding atmosphere should be essentially due to changes in voltage barrier heights between CCTO grains.

4. Conclusions

The study of processing variables allowed developing a new sol–gel synthesis procedure toward stable $CaCu_3Ti_4O_{12}$-precursor sols avoiding the precipitation of undesired compounds such as copper hydroxynitrate and copper(II) acetylacetonate. Ethanol and acetic acid are recommended as solvent and modifier of titanium tetraisopropoxide, respectively. The selected compositions, with PEG400 as linker and porogen, lead to the formation of mesoporous structures characterized by high porosity and surface-to-volume ratio, as indicated by the FE-SEM analysis. Highly homogeneous, continuous crystalline films were obtained by the proposed procedure. The $CaCu_3Ti_4O_{12}$ phase formation after the 700 °C annealing for 3 h was confirmed by XRD and Raman spectroscopy. The films, tested as gas sensors for oxygen, showed n-type conductivity, good sensitivity and relatively short response times. The electrical resistance changed by almost one decade in response to a change from nitrogen to oxygen atmosphere at the working temperature of 290 °C.

Acknowledgments

We thank Dr. S. Pellice and Dr. H. Romeo for their collaboration, and CONICET and SeCyT (Argentina), CNPq and Fapesp (Brasil) for the financial aid.

References

[1] A.P. Ramirez, M.A. Subramanian, M. Gardel, G. Blumberg, D. Li, T. Vogt, S.M. Shapiro, Solid State Commun. 115 (2000) 217–220.
[2] M.A. Subramanian, D. Li, N. Duan, B.A. Reisner, J. Solid State Chem. 151 (2000) 323–325.
[3] D.C. Sinclair, T.B. Adams, F.D. Morrison, A.R. West, Appl. Phys. Lett. 80 (2002) 2153–2155.
[4] P.R. Bueno, R. Tararam, R. Parra, E. Joanni, M.A. Ramírez, W.C. Ribeiro, E. Longo, J.A. Varela, J. Phys. D: Appl. Phys. 42 (2009) 055404.
[5] R. Lo Nigro, R.G. Toro, G. Malandrino, I.L. Fragalà, M. Losurdo, M.M. Giangregorio, G. Bruno, V. Raineri, P. Fiorenza, J. Phys. Chem. B 110 (2006) 17460–17467.
[6] (a) A. Rothschild, H.L. Tuller, J. Electroceram. 17 (2006) 1005–1012; (b) I.-D. Kim, A. Rothschild, T. Hyodo, H.L. Tuller, Nano Lett. 6 (2006) 193–198.
[7] E. Joanni, R. Savu, P.R. Bueno, E. Longo, J.A. Varela, Appl. Phys. Lett. 92 (2008) 132110.
[8] D. Fu, H. Taniguchi, T. Taniyama, M. Itoh, S.-ya. Koshihara, Chem. Mater. 20 (2008) 1694–1698.
[9] M.A. Ramirez, P.R. Bueno, J.A. Varela, E. Longo, Appl. Phys. Lett. 89 (2006) 212102.
[10] L.-T. Mei, H.-I. Hsiang, T.-T. Fang, J. Am. Ceram. Soc. 91 (2008) 3735–3737.
[11] C.-M. Wang, K.-S. Kao, S.-Y. Lin, Y.-C. Chen, S.-C. Weng, J. Phys. Chem. Solids 69 (2008) 608–610.
[12] S. Kwon, D.P. Cann, J. Electroceram., 2009, doi:10.1007/s10832-009-9563-1.
[13] D. Capsoni, M. Bini, V. Massarotti, G. Chiodelli, M.C. Mozzatic, C.B. Azzoni, J. Solid State Chem. 177 (2004) 4494–4500.
[14] S. Guillemet-Fritsch, T. Lebey, M. Boulos, B. Durand, J. Eur. Ceram. Soc. 26 (2006) 1245–1257.
[15] C. Masingboon, S. Maensiri, T. Yamwong, P.L. Anderson, S. Seraphin, Appl. Phys. A 91 (2008) 87–95.
[16] L.-C. Chang, D.-Y. Lee, C.-C. Ho, B.-S. Chiou, Thin Solid Films 516 (2007) 454–459.
[17] S. Jin, H. Xia, Y. Zhang, J. Guo, J. Xu, Mater. Lett. 61 (2007) 1404–1407.
[18] L. Liu, H. Fan, P. Fang, L. Jin, Solid State Commun. 142 (2007) 573–576.
[19] J. Liu, Y. Sui, C.G. Duan, R.W. Smith, W.N. Mei, J.R. Hardy, Chem. Mater. 18 (2006) 3878–3882.
[20] L. Feng, Y. Wang, Y. Yan, G. Cao, Z. Jiao, Appl. Surf. Sci. 253 (2006) 2268–2271.
[21] R. Jiménez, M.L. Calzada, I. Bretos, J.C. Goes, A.S.B. Sombra, J. Eur. Ceram. Soc. 27 (2007) 3829–3833.
[22] R. Parra, E. Joanni, J.W.M. Espinosa, R. Tararam, M. Cilense, P.R. Bueno, J.A. Varela, E. Longo, J. Am. Ceram. Soc. 91 (2008) 4162–4164.
[23] D.-L. Sun, A.-Y. Wu, S.-T. Yiny, J. Am. Ceram. Soc. 91 (2008) 169–173.
[24] D. Maurya, D.P. Singh, D.C. Agrawal, Y.N. Mohapatra, Bull. Mater. Sci. 31 (2008) 55–59.
[25] Y.W. Li, Z.G. Hu, J.L. Sun, X.J. Meng, J.H. Chu, J. Cryst. Growth 310 (2008) 378–381.
[26] P. Thomas, K. Dwarakanath, K.B.R. Varma, T.R.N. Kutty, J. Therm. Anal. Calorimetry 95 (2009) 267–272.
[27] Y.-S. Shen, B.-S. Chiou, C.-C. Ho, Thin Solid Films 517 (2008) 1209–1213.
[28] V.G. Kessler, G.I. Spijksma, G.A. Seisenbaeva, S. Håkansson, D.H.A. Blank, H.J.M. Bouwmeester, J. Sol–Gel Sci. Technol. 40 (2006) 163–179.
[29] (a) J. Livage, C. Sanchez, M. Henry, S. Doeuff, Solid State Ionics 32–33 (Part 2) (1989) 633–638;

(b) J.D. Wright, N.A.J.M. Sommerdijk, Sol–Gel Materials, Chemistry and Applications, CRC Press, Boca Raton, 2001.
[30] C. Sanchez, C. Boissière, D. Grosso, C. Laberty, L. Nicole, Chem. Mater. 20 (2008) 682–737.
[31] D.P. Birnie III, M. Manley, Phys. Fluids 9 (1997) 870–875.
[32] K. Kajihara, T. Yao, J. Sol–Gel Sci. Technol. 12 (1998) 185–192.
[33] S. Bu, C. Cui, X. Liu, L. Bai, J .Sol–Gel Sci.Technol. 43 (2007) 151–159.
[34] J.-G. Li, T. Ishigaki, X. Sun, J. Phys. Chem. C 111 (2007) 4969–4976.
[35] N. Kolev, R.P. Bontchev, A.J. Jacobson, V.N. Popov, V.G. Hadjiev, A.P. Litvinchuk, M.N. Iliev, Phys. Rev. B 66 (2002) 132102.
[36] D. Valim, A.G. Souza Filho, P.T.C. Freire, S.B. Fagan, A.P. Ayala, J. Mendes Filho, A.F.L. Almeida, P.B.A. Fechine, A.S.B. Sombra, J. Staun Olsen, L. Gerward, Phys. Rev. B 70 (2004) 132103.
[37] M.L. Moreira, E.C. Paris, G.S. do Nascimento, V.M. Longo, J.R. Sambrano, V.R. Mastelaro, M.I.B. Bernardi, J. Andrés, J.A. Varela, E. Longo, Acta Mater. 57 (2009) 5174–5185.
[38] Raman Spectra Database of Minerals and Inorganic Materials (RASMIN), AIST, December 2009 〈http://riodb.ibase.aist.go.jp/rasmin/E_index_list.html〉.
[39] G. Sakai, N.M. Baik, N. Miura, N. Yamazoe, Sens. Actuators B 77 (2001) 116–121.